ELSEVIER

Brachytherapy 13 (2014) 128–136

BRACHYTHERAPY

High-dose-rate prostate brachytherapy based on registered transrectal ultrasound and in-room cone-beam CT images

Aniek J.G. Even[1,2,4], Tonnis T. Nuver[1,3,4,*], Hendrik Westendorp[1,3], Carel J. Hoekstra[3], Cornelis H. Slump[2], André W. Minken[1,3]

[1]*Department of Medical Physics, Radiotherapeutic Institute RISO, Deventer, The Netherlands*
[2]*MIRA Institute for Biomedical Technology and Technical Medicine, University of Twente, Enschede, The Netherlands*
[3]*Department of Radiation Oncology, Radiotherapeutic Institute RISO, Deventer, The Netherlands*

ABSTRACT

PURPOSE: To present a high-dose-rate (HDR) brachytherapy procedure for prostate cancer using transrectal ultrasound (TRUS) to contour the regions of interest and registered in-room cone-beam CT (CBCT) images for needle reconstruction. To characterize the registration uncertainties between the two imaging modalities and explore the possibility of performing the procedure solely on TRUS.

METHODS AND MATERIALS: Patients were treated with a TRUS/CBCT-based HDR brachytherapy procedure. For 100 patients, dosimetric results were analyzed. For 40 patients, registration uncertainties were examined by determining differences in fiducial marker positions on TRUS and registered CBCT. The accuracy of needle reconstruction on TRUS was investigated by determining the position differences of needle tips on TRUS and CBCT. The dosimetric impact of reregistration and needle reconstruction on TRUS only was studied for 8 patients.

RESULTS: The average prostate V_{100} was 97.8%, urethra D_{10} was 116.3%, and rectum $D_{1\ cc}$ was 66.4% of the prescribed dose. For 85% of the patients, registration inaccuracies were within 3 mm. Large differences were found between needle tips on TRUS and CBCT, especially in cranial–caudal direction, with a maximum of 10.4 mm. Reregistration resulted in a maximum V_{100} reduction of 0.9%, whereas needle reconstruction on TRUS only gave a maximum reduction of 9.4%.

CONCLUSIONS: HDR prostate brachytherapy based on TRUS combined with CBCT is an accurate method. Registration uncertainties, and consequently dosimetric inaccuracies, are small compared with the uncertainties of performing the procedure solely based on static TRUS images. CBCT imaging is a requisite in our current procedure.

Keywords: Prostate; HDR brachytherapy; Transrectal ultrasound; Cone-beam CT; Registration

Introduction

High-dose-rate (HDR) brachytherapy is a well-established treatment option for localized prostate cancer. HDR brachytherapy has the ability to deliver a high dose per fraction in the clinical target volume, while sparing the surrounding tissue by a rapid dose falloff (1, 2). This highly conformal dose escalation seems an effective treatment method because a low α/β ratio is suggested for prostate cancer (3–5), indicating sensitivity to high dose per treatment fraction.

A wide variety in fractionation schemes and prescribed doses is described in the literature. HDR as a boost in combination with external beam radiation therapy (EBRT) is commonly applied in one to six fractions, HDR monotherapy most often in three to six fractions. There is no consensus on treatment schedules. In the literature reported treatment schemes provide comparable outcomes regarding tumor control and toxicity (6).

Also, the imaging modalities used during the procedures differ between institutes. Needle placement is usually

Received 25 March 2013; received in revised form 25 July 2013; accepted 1 August 2013.

All authors have no financial or other interest.

* Corresponding author. Department of Medical Physics, Radiotherapeutic Institute RISO, Nico Bolkesteinlaan 85, 7416SE Deventer, The Netherlands. Tel.: +31-570-6469-18; fax: +31-570-6469-17.

E-mail address: t.nuver@risomail.nl (T.T. Nuver).

[4] Both authors equally contributed to this manuscript.

1538-4721/$ - see front matter
http://dx.doi.org/10.1016/j.brachy.2013.08.001

performed under transrectal ultrasound (TRUS) guidance. Ultrasound is widely available, offers fast image acquisition, is easy to use, and costs are low. For treatment planning, CT, TRUS, or MRI is used (7).

CT is traditionally the most common imaging modality for HDR brachytherapy treatment planning. Needle reconstruction is accurate on CT images. However, organ delineation is difficult (8–10), and often, patients need to be transferred to and from a CT suite to acquire the images. Needle displacements might occur between CT planning and treatment, which can cause degradation of the dose distribution (11, 12). Catheter displacements larger than 1 cm were reported by Holly *et al.* (11).

TRUS-based HDR brachytherapy procedures provide more accurate prostate delineation (13). In addition, patients can remain in one room, and no additional CT or MRI treatment planning images are required. However, needle-tip localization on TRUS is reported to be uncertain (14, 15).

MRI provides good visualization of soft tissues and the needles and is potentially the optimal modality for treatment planning and needle guidance (16). Nevertheless, MRI in the operating theater is scarcely available, and examination costs are high.

At our institute, a novel HDR brachytherapy procedure was introduced that combines the advantages of TRUS and CT. TRUS and in-room C-arm cone-beam CT (CBCT) images are registered. TRUS images are used for organ delineation and CBCT images are used for needle reconstruction. Transfer of the patient to a separate CT room is not needed. The procedure was based on our successful ^{125}I approach (>1000 patients have been treated since 2007), earlier described by Westendorp *et al.* (17).

Holly *et al.* (11) also used a CBCT in their prostate HDR brachytherapy procedure. They used the CBCT images to verify that the catheters did not move, in a period typically of 2–3 h, between imaging in the CT room and treatment delivery in the treatment room. If considered necessary by the oncologist, catheter positions were adjusted.

The purpose of this study was to describe in detail the HDR procedure performed in our institute, characterize uncertainties in registration between TRUS and CBCT, and explore the possibility to perform the HDR procedure solely based on ultrasound.

Methods and materials

Patient and treatment characteristics

Between February 2010 and October 2012, 100 consecutive patients with high-risk prostate cancer were treated with EBRT and 2 weeks later with an HDR boost of 10 Gy. The patients had Stages T3a–b histologically proven prostate cancer and/or Gleason score >7. Patients with a prostate volume >60 cc after hormonal therapy and patients with a prostate-specific antigen level >100 ng/mL were excluded. The EBRT consisted of 20 fractions of 2.9 Gy tomotherapy. The prostate and seminal vesicles, with an additional margin of 7 mm, were defined as planning target volume (PTV). At the overlap of PTV and rectum or PTV and bladder, a dose gradient from 95% to 85% of the prescribed dose was applied. Four gold fiducial markers (Heraeus GmbH, Hanau, Germany) with a length of 5 mm and diameter of 1 mm had been inserted in the prostate for daily position verification using megavoltage CT.

The HDR brachytherapy procedure was based on the ^{125}I seeds implantation procedure performed at our institute (17). In a shielded operating theater, patients received spinal or general anesthesia. A Foley catheter was inserted, and the patient was placed in lithotomy position. Before inserting the HDR needles, usually one additional fiducial gold marker was inserted into the apical part of the prostate, as an anatomic landmark and for registration purposes. Two fixation needles (Medical Device Technologies, Gainesville, FL) were inserted into the central part of the prostate to fixate the prostate to the Martinez template (Nucletron, an Elekta company; Elekta AB, Stockholm, Sweden) which was mounted on an ultrasound EXII-Stepper (CIVCO, Kalona, IA). This was done under ultrasound guidance (Falcon 2101 EXL; BK Medical, Herlev, Denmark, February 2010 till January 2012; Flex Focus 400; BK Medical, January 2012 till October 2012; Endocavity Biplane Transducer 8848; BK Medical). After fixating the prostate to the template, a first set of transverse TRUS images was captured (US1). This image set is not disturbed by the HDR needles, and on these images, prostate and organs at risk are well visible. The trocar point stainless steel HDR needles (ø 1.5 × 200 mm; Nucletron, an Elekta company, Elekta AB) were inserted into the prostate, with the needle tips approximately 1 cm beyond the prostate base, and fixated to the Martinez template (Nucletron, an Elekta company). The template was then released from the stepper unit. Subsequently, a second set of TRUS images was acquired (US2) with the patient in semi-lithotomy position and reduced pressure of the US probe on the anterior rectal wall to prevent deformation of the prostate and the implant. This second set of US images is used in treatment planning. The TRUS images were either manually saved every 2.5 mm or automatically acquired with 1 mm steps.

Transfer tubes were connected between the HDR needles and the afterloader. Thereafter, the patient was repositioned. The TRUS probe and leg supports were removed, an extension was mounted on the operating couch, and the patient's knees were placed on foam cushions. CBCT images were acquired (Siemens Arcadis Orbic 3D; Siemens Medical Systems, Erlangen, Germany). The CBCT images were reconstructed with a slice thickness of 1 mm at 1-mm interval. The HDR needles and the gold markers were well visible on these CBCT images.

The three-dimensional TRUS and CBCT data sets were transferred to the treatment planning system (Flexiplan V2.5; Nucletron, an Elekta company, Elekta AB). Contouring of the prostate, urethra, rectum, and bladder was performed on US2 by two radiation oncologists. TRUS images without HDR needles (US1) were used to verify the contours. The urethra was contoured generously to add a safety margin. Also, a microboost region was roughly contoured. This region, with the dominant lesion, was determined based on pre-treatment MRI, histology findings, and digital rectal examination. A registration was performed between the US2 and the CBCT images. One (or two) fiducial markers and four (or three) clearly distinguishable needle tips (two posterior and two anterior) were selected on both imaging modalities. The corresponding points were registered using least squares distance optimization. The quality of the registration was visually checked by inspecting the complete needle/marker configuration. Needle tips were used since, because of the HDR needles, insufficient markers were visible on US2 to perform the registration solely based on markers. Then, each needle was reconstructed on CBCT by identifying the tip and a position below the prostate apex. The CBCT images were also used to verify the delineated urethra: Radiopaque contrast agent was injected into the Foley catheter.

Finally, dwell positions and dwell times were calculated to create a dose distribution based on the needle positions and organ contours. It was aimed to create a dose distribution with prostate V_{100} >97% of the prescribed dose, prostate V_{200} <15%, conformity index (COIN; Eq. 3 in Ref. (18)) >0.68, urethra D_{max} <125%, urethra D_{10} <120%, rectum D_{max} <100%, rectum $D_{1\ cc}$ <70%, and boost V_{150} as high as possible, taken into account the other constraints. The dose distribution was achieved via inverse planning dose optimization (IPSA (19)), followed by manual fine tuning.

Before starting irradiation, several checks were performed. An anterior–posterior (AP) x-ray image was acquired of the HDR implant before and after the planning procedure. On both AP images, several fiducial markers were localized, and registration was performed to verify that the needles had not moved between the moment of imaging and the actual treatment delivery. Consistency between the data of the treatment planning computer and the treatment delivery unit was checked. In addition, the total reference air kerma (TRAK) multiplied with the COIN was plotted vs. the prostate volume, as described by Huckle *et al.* (20), to verify the consistency of the treatment plan. Eventually, after performing all checks successfully, the treatment plan was transferred to the afterloader (Flexitron; Nucletron, an Elekta company, Elekta AB) and irradiation was started.

The total duration of the procedure was timed for 42 patients. For 15 of these patients, this timing was also done for the different steps in the procedure to determine if time could be gained.

Registration uncertainties

To examine the registration uncertainties between TRUS and CBCT, images of in total 40 patients were analyzed. A group of 20 patients (treated between June 2011 and March 2012) scanned with a TRUS slice spacing of 2.5 mm and a second group of 20 patients (treated between May 2012 and September 2012) scanned with a TRUS slice spacing of 1 mm were included. For each patient, one marker was selected on the CBCT images using our treatment planning system Flexiplan (Nucletron, an Elekta company). In general, a marker near the apex was chosen as these were clearly distinguishable, both on TRUS and CBCT. The coordinates of the center of that marker were then determined on US2 and thereafter on CBCT images by a first observer (AJGE). The difference in marker position was calculated by subtracting the position on CBCT from the position on US2. The marker identification on TRUS and CBCT was repeated by a second observer (TTN) for the same marker.

In SPSS (V20.0.0; International Business Machines Corporation, Armonk, NY), a student *t* test was performed to compare the marker locations determined by the first and second observers. Thereafter, an average fiducial marker position difference between US2 and CBCT was calculated from the data of the two observers. These average differences were split into a 2.5- and 1-mm slice spacing group. A student *t* test was performed to compare the results of both groups.

Needle-tip positions

The accuracy of needle localization on TRUS images was evaluated by determining the position of all needle-tips for a patient on TRUS and subsequently on the registered CBCT. Needle-tip position differences were determined by subtracting the positions on CBCT from the positions on TRUS. The same 40 patients and in total 709 needles (13–23 per patient) were analyzed. The distributions of the 2.5- and 1-mm groups were tested for significant differences.

Reproducibility tests

To assess the uncertainties in needle-tip determination and uncertainties in registration, additional analyses were performed for 4 patients with relatively large differences in needle-tip positions and 4 patients with relatively large differences between the fiducial marker positions on TRUS and CBCT. For the 8 patients, coordinates of needle tips on CBCT and TRUS images were determined twice by the same observer (AJGE), and the variation between both analyses was calculated. Also, registration was performed twice. Needle-tip coordinates after the first and second registrations were determined on the registered CBCT images, and the results were compared. The first and

second series of analyses were separated by more than a month.

Effect of needle positions on dose distribution

For the same 8 patients, the potential effect of shifted needle positions on the dose distribution was investigated. First, the applicators were repositioned according to the coordinates of the needles on the CBCT scans after the second registration. The dose distribution was recalculated and compared with the original distribution. Also, applicators were placed as determined on TRUS images (US2), and doses were recalculated. For all dose distributions, the contours of the organs remained the same, and the dwell times and positions in the needles remained unchanged.

Results

The dosimetry data of the first 100 patients treated in our institute are shown in Table 1. The graph with TRAK × COIN plotted against prostate volume, which is used for treatment verification, is depicted in Fig. 1. Our data were normalized to a prescribed dose of 15 Gy to facilitate the comparison with Huckle *et al.* (20).

The mean duration of our procedure was 3.5 h. Preparing the patient for the procedure took on average 0.5 h, placing (fixation) needles and acquiring TRUS and CBCT images 1 h, the planning part of the procedure 1.5 h, and irradiation and wrapping up the procedure on average 0.5 h.

In Fig. 2, fiducial marker position differences between TRUS and CBCT are depicted for the 2.5- and 1-mm TRUS slice spacing groups. For the right–left (RL) direction, all registration uncertainties were within 2 mm; for posterior–anterior (PA) direction, 90% were within 2 mm; and for cranial–caudal (CC) direction, 67.5% of the differences were within 2 mm. For 85% of the patients, the total registration inaccuracies were within 3 mm. For 1 of the 40 fiducial markers, position differences determined by the second

Table 1
HDR brachytherapy dosimetry data for 100 consecutive patients

Observables	Results
Volume of CTV (cc)	32 (18–60)
Needles	17 (12–25)
V_{100} (%)	97.8 (89.3–99.7)
V_{200} (%)	11.2 (8.0–17.4)
COIN	0.71 (0.57–0.81)
Urethra D_{max} (%)	123.1 (114.8–231.0[a])
Urethra D_{10} (%)	116.3 (106.8–126.8)
Rectum D_{max} (%)	87.7 (71.6–133.7)
Rectum $D_{1\ cc}$ (%)	66.4 (52.3–78.3)
Boost V_{150} (%)	70.0 (37.0–90.0)

HDR = high-dose-rate; CTV = clinical target volume; COIN = conformity index.

Median values and range. Prescribed dose to CTV 10 Gy.

[a] Second highest urethra max dose was 148.2%.

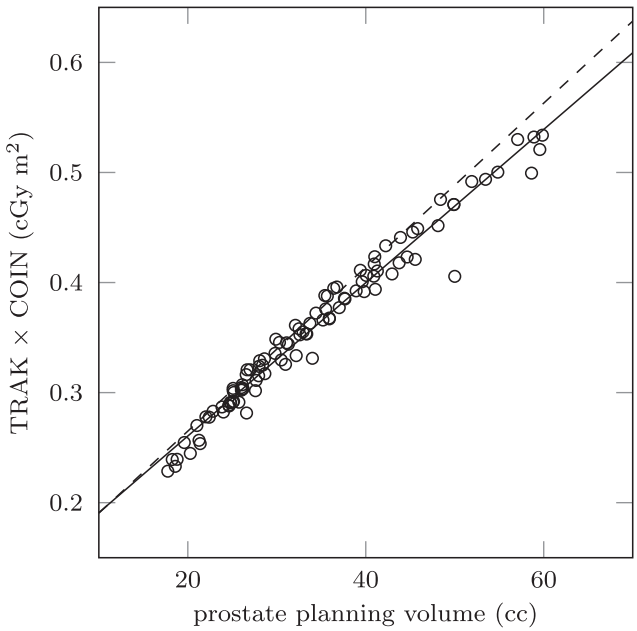

Fig. 1. Verification of the output of the treatment planning system. Depicted values are for a prescribed dose of 15 Gy. A linear fit ($y = 0.00696x + 0.121$) was applied for the 100 patients (solid line). The dashed line represents the correlation ($y = 0.00745x + 0.116$) determined by Huckle *et al.* (20). TRAK = total reference air kerma; COIN = conformity index.

observer were selected instead of an average value. For this marker, a total difference of 3.9 mm was found between the two observers. Two marker-like structures were visible on TRUS images, and in retrospect, it was concluded that the first observer had mistaken an artifact for the fiducial marker.

On TRUS images, differences between the fiducial marker positions determined by the first and second observers were on average −0.1 ± 0.3 (1 standard deviation [SD]), −0.1 ± 0.3 (1 SD), and +0.1 ± 0.7 (1 SD) mm for RL, PA, and CC directions, respectively. On the CBCT images, the average differences were −0.1 ± 0.2 (1 SD), 0.0 ± 0.1 (1 SD), and −0.1 ± 0.2 (1 SD) mm, respectively. Although the differences were very small, the student *t* test showed that these differences were significant for both the RL and the CC directions for the CBCT images. For the fiducial marker position differences between US2 and CBCT, no significant variation was found ($p > 0.05$) between the 1- and 2.5-mm TRUS slice spacing groups.

In Fig. 3, position differences between needle-tip coordinates on TRUS and CBCT are shown. For the 2.5-mm slice spacing group, average position differences of 0.0 ± 1.5 (1 SD), +0.1 ± 1.0 (1 SD), and +0.3 ± 3.0 (1 SD) mm were found for the RL, PA, and CC directions, respectively. For the 1-mm slice spacing group, average position differences of +0.2 ± 1.3 (1 SD), 0.0 ± 0.9 (1 SD), and 0.0 ± 2.3 (1 SD) mm were found for RL, PA, and CC directions, respectively. The largest differences were seen in CC

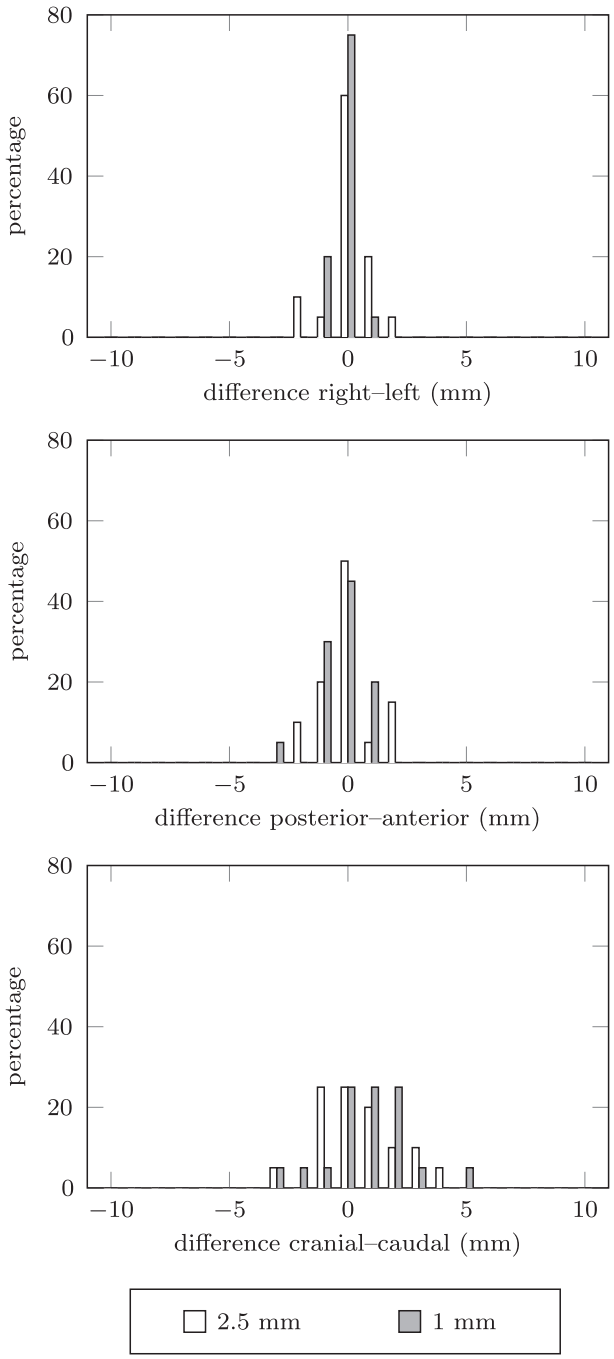

Fig. 2. Fiducial marker position differences for 20 patients scanned with 2.5-mm TRUS slice spacing and 20 patients scanned with 1-mm spacing. Differences were calculated by subtracting the position of the center of the marker on CBCT from the marker position on TRUS. TRUS = transrectal ultrasound; CBCT = cone-beam CT.

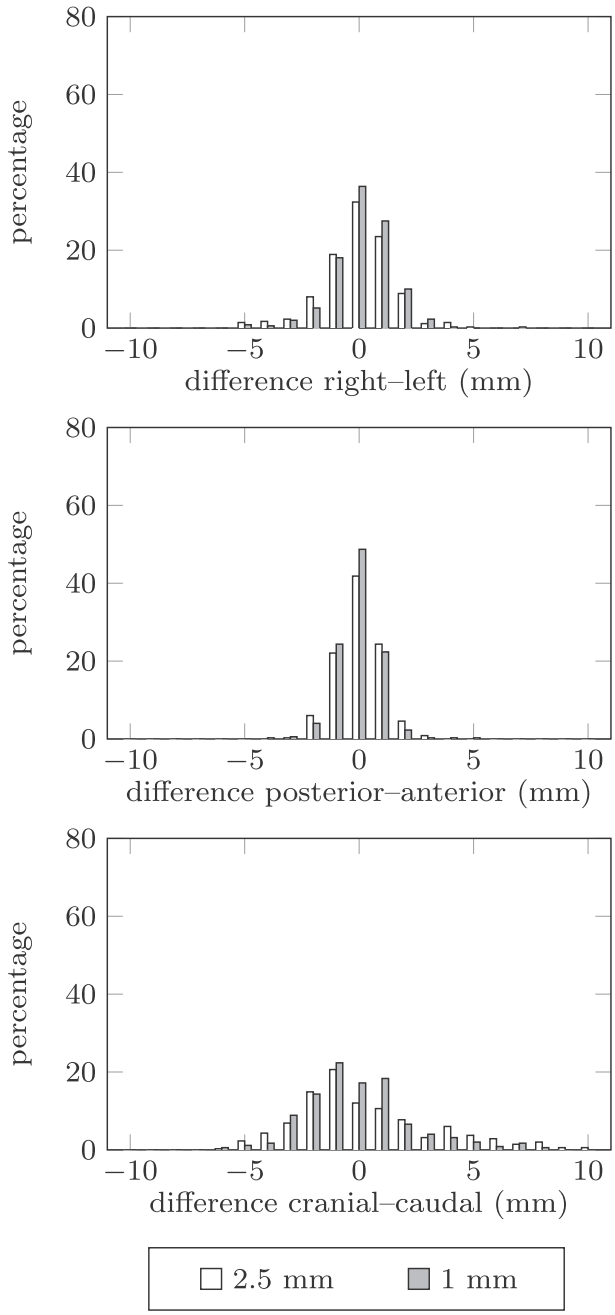

Fig. 3. Needle-tip position differences for 20 patients scanned with 2.5 mm (349 needles) and 20 patients scanned with 1 mm (360 needles) step size TRUS. Differences were calculated by subtracting the needle-tip coordinates determined on CBCT images from the coordinates on TRUS images. TRUS = transrectal ultrasound; CBCT = cone-beam CT.

direction: 10.4 mm for the 2.5-mm group and 8.5 mm for the 1-mm group. The maximum differences were 5.4 and 7.2 mm in RL direction and 3.5 and 4.8 mm in PA direction, respectively. In the CC direction, the largest position differences were observed for needles for which needle tips were localized on TRUS more caudally than on CBCT. No significant difference was found between the mean position differences of the 2.5- and 1-mm slice spacing groups ($p > 0.05$) for RL, PA, and CC directions. However, in CC direction, the SD of the 2.5-mm group was significantly larger ($p < 0.01$) than that of the 1-mm group.

For the 8 patients for whom the needle-tip positions were determined a second time, both on TRUS and CBCT, and for whom the registration between TRUS and CBCT was repeated, the results are shown in Fig. 4. As can be

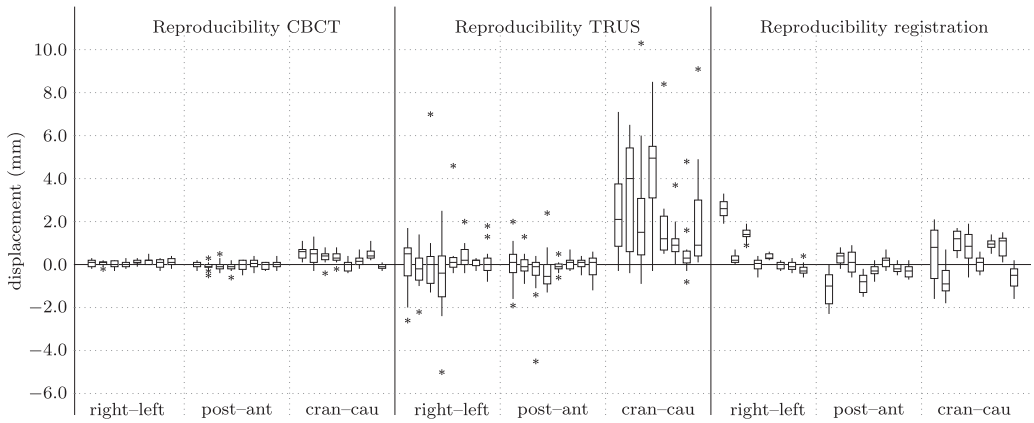

Fig. 4. Box plots displaying the reproducibility of determining needle tips in the same scan twice. Position difference is defined as coordinates of the first needle-tip selection minus the second set of coordinates. On the left, the reproducibility box plots for CBCT are given; in the middle, the reproducibility box plots for TRUS are given; and on the right, the difference of CBCT needle-tip positions between two registrations is given. Eight patients were analyzed, and the results are divided into RL, PA, and CC directions. The boxes cover the area between the 25th and 75th percentiles. Whiskers are the adjacent values between the edges of the box and 1.5 times the length of the box. All outliers are displayed as asterisk. CBCT = cone-beam CT; TRUS = transrectal ultrasound; RL = right–left; PA = posterior–anterior; CC = cranial–caudal.

seen in the figure, the largest uncertainties were found for the identification of the needle tips on TRUS, especially in CC direction (middle panel). Differences up to 10 mm were seen. Very small differences (<1 mm) were seen between the needle identifications on CBCT (left panel) and also the reregistrations (right panel) showed limited change in needle-tip positions (<2 mm).

In Table 2, the effect on the dose distribution parameters of the reregistration and the reconstruction of the needles on TRUS is tabulated for the 8 patients. Table 2 shows, for each patient, the dosimetric parameters of the plans as follows: first row (clinical): plan used for treatment; second row (Reg_2): after reregistration of the CBCT and US2; and third row (TRUS): needles reconstructed solely based on US2. Minor differences were seen between the clinical plan and the second registration for prostate V_{100}, urethra D_{10}, and rectum $D_{1\ cc}$. For prostate V_{100}, an average difference between the two dose distributions of −0.3% was observed, with a maximum difference of −0.9%. For urethra D_{10}, a mean difference of +1.3% and a maximum difference of +5.4% were found, and for rectum $D_{1\ cc}$, on average −0.8% and a maximum difference of −4.2%. The influence of the inaccuracies in needle reconstruction on TRUS was clearly larger: For prostate V_{100}, an average difference between the clinical plan and the TRUS plan of −2.6% was found, with a maximum difference of −9.4%. For urethra D_{10}, these numbers were +9.4% on average and a maximum deviation of +15.5%, and for rectum $D_{1\ cc}$, +4.3% on average and a maximum of +11.5%.

Discussion

In this study, a novel HDR brachytherapy procedure was described combining the advantages of TRUS and CT. It facilitates precise contouring of the regions of interest on TRUS and calculation of an exact dose distribution based on highly accurate needle reconstruction on CBCT. For the first 100 treated patients, dosimetric results comparable with the results of the group of Morton *et al.* (21) were achieved.

A similar linear relation was found between the prostate volume and the product of TRAK and COIN as reported by Huckle *et al.* (20). However, the outlier in Fig. 1, for a planning volume of 50 cc, indicates that the model is not valid for all patients. The outlier patient had a relatively low V_{100} (89.9%) that caused the deviation from the linear relationship. Plotting TRAK × COIN divided by V_{100} against prostate planning volume removed the outlier and yielded a stronger correlation $R^2 = 0.982$ ($y = 0.00721x + 0.123$). For the TRAK × COIN model, a R^2 of 0.972 was found.

The registration that has to be performed between the two imaging modalities is a source of uncertainty. The analysis comparing fiducial marker positions on TRUS and CBCT showed, for the majority of patients, that deviations were smaller than 2 mm. For the 40 analyzed patients, only 2 patients had a marker position difference in CC direction exceeding 3 mm. For both patients, an additional marker was analyzed, and a decrease in registration uncertainty was observed for the second analyzed marker (from 3.8 to −0.6 and 4.6 to −1.3 mm). A possible reason for the initial large position difference for 1 of the 2 patients was the location of the marker: The marker seemed to be outside the prostate and may have moved independently of the prostate between TRUS and CBCT scanning. No explanation was found for the other patient. Reregistration of both patients (last 2 patients in right panel of Fig. 4) only showed small position changes (<1 mm).

The effect of needle displacements on prostate coverage and irradiation of organs at risk was analyzed

Table 2
Difference in dose distribution between the original needle-tip locations (Clinical), needle positions based on the second registration (Reg_2), and needle-tip locations based on TRUS images (TRUS)

	V_{100}	V_{200}	COIN	Urethra D_{max}	Urethra D_{10}	Rectum D_{max}	Rectum $D_{1\ cc}$	Boost V_{150}
Patient 1								
Clinical	98.0	10.5	0.632	124.1	115.8	85.5	67.3	82.5
Reg_2	98.3	11.2	0.636	143.4	121.2	91.9	69.8	86.7
TRUS	99.2	17.5	0.658	136.9	127.6	96.1	71.4	92.2
Patient 2								
Clinical	94.4	17.0	0.727	123.7	117.2	82.4	62.4	75.7
Reg_2	94.6	17.8	0.732	127.5	120.9	79.0	60.8	72.3
TRUS	89.3	16.4	0.654	138.1	132.7	106.3	69.7	56.0
Patient 3								
Clinical	94.2	12.4	0.727	138.2	117.2	93.6	66.6	63.8
Reg_2	93.5	12.2	0.716	131.3	117.7	90.8	65.6	65.3
TRUS	86.2	11.0	0.617	342.3	127.4	108.0	73.5	65.7
Patient 4								
Clinical	98.5	13.8	0.673	120.3	115.8	112.8	71.9	72.6
Reg_2	98.0	13.9	0.672	118.7	114.7	135.0	75.5	74.0
TRUS	89.1	15.3	0.564	151.0	124.2	170.0	83.4	83.3
Patient 5								
Clinical	97.2	9.8	0.710	123.4	115.4	94.6	65.2	53.5
Reg_2	97.0	10.0	0.707	125.9	116.2	156.0	61.0	50.9
TRUS	97.9	12.1	0.722	137.8	126.4	100.1	64.9	71.8
Patient 6								
Clinical	98.1	8.6	0.688	119.9	113.0	92.0	68.5	84.1
Reg_2	97.2	7.9	0.672	124.9	111.2	90.3	66.7	80.2
TRUS	97.8	9.8	0.688	134.4	118.4	95.0	69.1	85.2
Patient 7								
Clinical	98.2	8.9	0.643	131.0	115.6	92.7	65.2	
Reg_2	98.3	8.9	0.644	148.6	117.9	89.6	64.3	
TRUS	97.9	9.6	0.647	155.4	119.3	98.7	69.1	
Patient 8								
Clinical	97.2	8.8	0.688	137.8	120.5	91.0	70.0	68.6
Reg_2	96.7	8.5	0.681	162.0	121.4	86.4	67.2	72.2
TRUS	97.7	9.0	0.699	157.0	129.3	90.5	70.0	66.6

TRUS = transrectal ultrasound; COIN = conformity index.

All values, except the COIN, are percentages of prescribed dose. For patient 7, no boost region was defined.

by Kolkman-Deurloo *et al.* (12). They simulated a displacement of the entire implant in CC direction of 3, 5, 7, and 10 mm and concluded that for implants with displacements smaller than 3 mm, the quality of the dose distribution did not change significantly. If one assumes that the deviation in CC fiducial marker position equals the error in needle point positions in our procedure, it can be concluded that the registration uncertainty does not significantly influence the quality of the dose distribution.

Reregistration of TRUS and CBCT showed minor influence on the dose distribution parameters (prostate V_{100}, rectum $D_{1\ cc}$, and urethra D_{10}), as can be seen in Table 2. This also supports our conclusion that the registration uncertainty has minor impact on the quality of the dose distribution.

Our analysis in which we determined needle-tip positions on TRUS (US2) showed relatively large deviations with respect to the positions determined on CBCT (Fig. 3). The dominant deviations were seen in CC direction. Deviations up to 10 mm were seen. Although registration inaccuracies will have contributed to these deviations, our results for the fiducial marker positions, which show much smaller deviations, indicate that the dominant source of deviation is the difficulty in identifying needle tips on TRUS. This is supported by the results in Fig. 4 (middle panel) that show large differences between the initially identified needle tips on TRUS and the positions that were identified a second time by the same observer more than 1 month after the first identification. Significant differences were seen for not only the CC direction but also the RL and to a lesser extent for the PA direction. For the CC direction, the needle-tip positions in the second analysis were systematically identified more cranially than in the first identification. Especially for the first 4 patients, with large deviations in the initially identified needle positions, the needles were identified more cranially in the second analysis. No direct reason could be identified for this difference. However, it might be related to our initial finding that needles on CBCT were identified more cranially than those on TRUS and that this knowledge may have resulted in a bias in the second identification.

Our results are supported by the phantom studies of Schmid *et al.* (15) and Zheng *et al.* (14). Schmid reported errors up to 5.8 mm for needle-tip identification on TRUS in CC direction and Zheng found deviations larger than 10 mm.

Although it was expected that reducing the TRUS step size from 2.5 to 1 mm would improve the accuracy of our procedure, no significant changes were seen in the analysis of the fiducial marker positions. The inherent uncertainty is half a step size. The accuracy gain going from 2.5 to 1.0 mm step size seems to be small compared with the registration accuracy and the accuracy of identifying needle tips and fiducial markers on TRUS.

One of the goals of this study was to examine the possibility of reducing the time of the procedure by using only one imaging modality, TRUS. Based on the timing results for our procedure, it was estimated that leaving out the CBCT would potentially reduce the overall treatment time by 30 min. Especially in CC direction, however, large uncertainties were observed in needle reconstruction, which would potentially result in a clinically not acceptable dose distribution. Therefore, to ensure the quality of our procedure, CBCT imaging remains a necessity in combination with static TRUS imaging. Moreover, the CBCT images have the additional advantage that they provide an independent verification of the geometric integrity (step size and calibration) of the US images.

Performing HDR brachytherapy solely based on TRUS images requires an additional verification of the positions of the needles. Measuring the protrusion lengths of the needles, as suggested by several authors (14, 15), seems a promising method. This study shows that for TRUS, not only in the CC direction needle reconstruction uncertainties

exist but also that these have to be considered in the RL and to a lesser extent the PA direction.

Catheter displacement between the moment of imaging/planning and the treatment delivery is of concern in prostate HDR brachytherapy. Various authors (11, 22–25) reported (predominantly) caudal displacements ranging from a few millimeters to 2 cm. This resulted in degradation of the brachytherapy dose distribution (22, 24). Displacements were attributed to template movement, internal prostate movement, and tissue edema between the prostate apex and the perineum. Most of these studies considered interfraction needle displacements and/or involved moving the patient to and from a CT suite (11, 24). In all studies, flexible catheters were used, and generally, the template was sutured to the patient's skin. In our procedure, which consists of a single irradiation fraction, the time between imaging and treatment delivery is only 1.5 h, the position change of the patient between US and CBCT imaging is very limited, and rigid metal needles are used. Moreover, two fixation needles are used to attach the prostate to the Martinez template (Nucletron, an Elekta company) and thereby prevent the movement of the needles with respect to the prostate. Pieters *et al.* (26) showed for their pulsed-dose-rate brachytherapy procedure that, with the use of self-anchoring catheters, the average displacement of the implant over a 3-day period was only 1.2 mm. Figure 3 shows for a large number of needles that the tips are identified more cranially than on US2, which clearly does not correspond to a caudal needle movement. No evidence was found for rotation of the template around a fulcrum, as was observed by Kim *et al.* (23). Additionally, AP x-ray images of the implant obtained directly after imaging and before treatment delivery were visually inspected and never revealed any (significant) movement of the needles with respect to the gold markers inside the prostate. Therefore, the needle displacement is not expected to be of major impact on the quality of our treatment or on the conclusions of this study.

Seppenwoolde *et al.* (27) studied the possibility to use a TRUS-based HDR brachytherapy plan, with the patient in lithotomy position and US probe in the rectum, for subsequent treatment fractions with the patient in a different position (lowered legs) and without US probe. They found relocation of the catheters and changes in the shape of the prostate and the rectum. In our procedure, the needles are imaged (CBCT) when the patient is in the treatment position, and relocation of the needles is not observed. The delineation of the urethra is checked in the registered CBCT scan. To prevent deformation of the prostate, the pressure of the US probe on the anterior rectal wall is reduced for US2. Potentially, as a result of the absence of the US probe, the rectal wall, which was delineated on US2, might be further away from the prostate during treatment. This will result in a lower dose to the rectum than planned, as was shown by Seppenwoolde *et al.* (27).

Conclusions

A successful HDR brachytherapy procedure is described in this article combining the advantages of the image properties of TRUS and CBCT. Contouring is performed on TRUS, and dose calculation is based on highly accurate needle reconstruction on CBCT. The registration uncertainties of this procedure are proven to be small and have minor impact on the prostate coverage and dose to the organs at risk. Major deviations were reported, especially in CC direction, for the reconstruction of the needles on TRUS images, resulting in substantial uncertainties in the dose distributions. Therefore, CBCT imaging is a requisite in our current procedure.

References

[1] Koukourakis G, Kelekis N, Armonis V, *et al*. Brachytherapy for prostate cancer: A systematic review. *Adv Urol* 2009;327945.
[2] Mahmoudieh A, Tremblay C, Beaulieu L, *et al*. Anatomy-based inverse planning dose optimization in HDR prostate implant: A toxicity study. *Radiother Oncol* 2005;75:318–324.
[3] Brenner DJ, Martinez AA, Edmundson GK, *et al*. Direct evidence that prostate tumors show high sensitivity to fractionation (low α/β ratio), similar to late-responding normal tissue. *Int J Radiat Oncol Biol Phys* 2002;52:6–13.
[4] Fowler J, Chappell R, Ritter M. Is α/β for prostate tumors really low? *Int J Radiat Oncol Biol Phys* 2001;50:1021–1031.
[5] Nath R, Bice WS, Butler WM, *et al*. AAPM recommendations on dose prescription and reporting methods for permanent interstitial brachytherapy for prostate cancer: Report of Task Group 137. *Med Phys* 2009;36:5310–5322.
[6] Yamada Y, Rogers L, Demanes DJ, *et al*. American Brachytherapy Society consensus guidelines for high-dose-rate prostate brachytherapy. *Brachytherapy* 2012;11:20–32.
[7] Kovács G, Pötter R, Loch T, *et al*. GEC/ESTRO-EAU recommendations on temporary brachytherapy using stepping sources for localised prostate cancer. *Radiother Oncol* 2005;74:137–148.
[8] Rasch C, Barillot I, Remeijer P, *et al*. Definition of the prostate in CT and MRI: A multi-observer study. *Int J Radiat Oncol Biol Phys* 1999;43:57–66.
[9] Usmani N, Sloboda R, Kamal W, *et al*. Can images obtained with high field strength magnetic resonance imaging reduce contouring variability of the prostate? *Int J Radiat Oncol Biol Phys* 2011;80:728–734.
[10] Smith WL, Lewis C, Bauman G, *et al*. Prostate volume contouring: A 3D analysis of segmentation using 3DTRUS, CT, and MR. *Int J Radiat Oncol Biol Phys* 2007;67:1238–1247.
[11] Holly R, Morton GC, Sankreacha R, *et al*. Use of cone-beam imaging to correct for catheter displacement in high dose-rate prostate brachytherapy. *Brachytherapy* 2011;10:299–305.
[12] Kolkman-Deurloo IK, Roos MA, Aluwini S. HDR monotherapy for prostate cancer: A simulation study to determine the effect of catheter displacement on target coverage and normal tissue irradiation. *Radiother Oncol* 2011;98:192–197.
[13] Liu D, Usmani N, Ghosh S, *et al*. Comparison of prostate volume, shape, and contouring variability determined from preimplant magnetic resonance and transrectal ultrasound images. *Brachytherapy* 2012;11:284–291.
[14] Zheng D, Todor DA. A novel method for accurate needle-tip identification in trans-rectal ultrasound-based high-dose-rate prostate brachytherapy. *Brachytherapy* 2011;10:466–473.
[15] Schmid M, Crook JM, Batchelar D, *et al*. A phantom study to assess accuracy of needle identification in real-time planning of

ultrasound-guided high-dose-rate prostate implants. *Brachytherapy* 2013;12:56–64.

[16] Lakosi F, Antal G, Vandulek C, *et al*. Open MR-guided high-dose-rate (HDR) prostate brachytherapy: Feasibility and initial experiences. *Pathol Oncol Res* 2011;17:315–324.

[17] Westendorp H, Hoekstra CJ, van't Riet A, *et al*. Intraoperative adaptive brachytherapy of iodine-125 prostate implants guided by C-arm cone-beam computed tomography-based dosimetry. *Brachytherapy* 2007;6:231–237.

[18] Baltas D, Kolotas C, Geramani K, *et al*. A conformal index (COIN) to evaluate implant quality and dose specification in brachytherapy. *Int J Radiat Oncol Biol Phys* 1998;40:515–524.

[19] Pouliot J, Kim Y, Lessard E, *et al*. Inverse planning for HDR prostate brachytherapy used to boost dominant intraprostatic lesions defined by magnetic resonance spectroscopy imaging. *Int J Radiat Oncol Biol Phys* 2004;59:1196–1207.

[20] Huckle A, Al-Qaisieh B, Bownes P. Methods of verifying the output of the treatment planning system used for high dose rate (HDR) prostate brachytherapy. *Radiother Oncol* 2012;103:261–265.

[21] Morton GC, Loblaw DA, Sankreacha R, *et al*. Single-fraction high-dose-rate brachytherapy and hypofractionated external beam radiotherapy for men with intermediate-risk prostate cancer: Analysis of short- and medium-term toxicity and quality of life. *Int J Radiat Oncol Biol Phys* 2010;77:811–817.

[22] Foster W, Cunha AM, Hsu IC, *et al*. Dosimetric impact of interfraction catheter movement in high-dose rate prostate brachytherapy. *Int J Radiat Oncol Biol Phys* 2011;80:85–90.

[23] Kim Y, Hsu IC, Pouliot J. Measurement of craniocaudal catheter displacement between fractions in computed tomography-based high dose rate brachytherapy of prostate cancer. *J Appl Clin Med Phys* 2007;8:2415–2427.

[24] Simnor T, Li S, Lowe G, *et al*. Justification for inter-fraction correction of catheter movement in fractionated high dose-rate brachytherapy treatment of prostate cancer. *Radiother Oncol* 2009;93:253–258.

[25] Whitaker M, Hruby G, Lovett A, *et al*. Prostate HDR brachytherapy catheter displacement between planning and treatment delivery. *Radiother Oncol* 2011;101:490–494.

[26] Pieters BR, van der Grient JN, Blank LE, *et al*. Minimal displacement of novel self-anchoring catheters suitable for temporary prostate implants. *Radiother Oncol* 2006;80:69–72.

[27] Seppenwoolde Y, Kolkman-Deurloo IK, Sipkema D, *et al*. HDR prostate monotherapy—Dosimetric effects of implant deformation due to posture change between TRUS- and CT-imaging. *Radiother Oncol* 2008;86:114–119.